Investigation of atomic and electronic structure of primitive and synthesized amorphous silicates using high-resolution electron energy-loss spectroscopy (HREELS). J. P. Bradley, Institute of Geophysics and Planetary Physics, Lawrence Livermore National Laboratory, bradley33@llnl.gov.

Introduction: Amorphous silicates are dominant solids in the interstellar medium, the outer regions of accretion disks around some young stars, and in chondritic porous interplanetary dust particles (CP IDPs) that are believed to be from small, cold outer solar system bodies. Thus, amorphous silicates include some of the most chemically and isotopically primitive objects available for laboratory investigations, but ironically, they also lie at the frontier of meteoritic materials characterization. The challenge amorphous silicates present is that, compared to crystalline silicates, there are far fewer indicators of how they formed. In the absence of specific indicators, non-equilibrium condensation is the often-assumed formation mechanism.

X-ray absorption near-edge structure (XANES) and extended x-ray absorption fine structure (EXAFS) are powerful synchrotron-based techniques for examining valence band structure, local bonding and atomic arrangements in amorphous silicates [1]. Analogous electron energy-loss near-edge structure (ELNES) and extended energy-loss fine structure (EXELFS) are also used to probe the properties of amorphous silicates [2]. These electron beam methods offer orders of magnitude better spatial resolution, but their application has been limited in the past by ~10× poorer energy resolution, ~1 eV for ELNES and EXELFS versus ~0.1 eV for XANES and EXAFS. Using a (scanning) transmission electron microscope (80-300 keV FEI high-base Titan STEM) equipped with a monochromator, high-resolution electron energy loss spectroscopy (HREELS) measurements with ~0.1 eV energy resolution are now possible [3-5]. We are using monochromated STEM to characterize and compare the properties of amorphous silicates formed by astrophysically relevant mechanisms, including shock, non-equilibrium vapor phase condensation, irradiation exposure and precipitation from liquids and fluids. Here the properties of amorphous silicates produced by vapor phase condensation and irradiation of crystalline silicates are compared with those of amorphous silicates (GEMS) in IDPs.

Experimental: Amorphous silicates ($MgSiO_x$) condensed from the vapor phase under non-equilibrium conditions were produced in the condensation smokes apparatus in J. Nuth's laboratory at NASA Goddard, where gas-phase precursors such as silane (SiH_4) are introduced into an atmosphere dominated by hydrogen at ~90 Torr at temperatures between 500 and 1500K. Magnesium metal is introduced in a graphite crucible and an oxidant is introduced separately. The starting materials undergo combustion and, upon exiting the furnace, they are rapidly quenched and condense onto a metal plate [6].

Condensed amorphous silicates were embedded in epoxy and thin-sectioned using an ultramicrotome equipped with a diamond knife. The properties of the amorphous silicates were compared with amorphous silicates known as GEMS (glass with embedded metals and sulfides) in several CP IDPs. End-member MgSiOx rather than (Mg,Fe)SiOx condensates were selected for the comparison because the amorphous Mg-silicate matrices of GEMS are essentially iron free [7,8].

Thin sections were examined using the monochromated and aberration-corrected STEM. The compositions of the non-equilibrium condensates were measured using energy-dispersive x-ray spectroscopy (EDX) and structural and electronic properties of the samples were investigated using high-resolution electron energy-loss spectroscopy (HREELS). Two energy-loss regions were examined with energy resolution between 0.1 and 0.5 eV, the 100-150 eV regions that contains the Si-$L_{2,3}$ core scattering edge and the low-loss 0-35 eV containing the zero-loss, valence band and plasmon scattering regions.

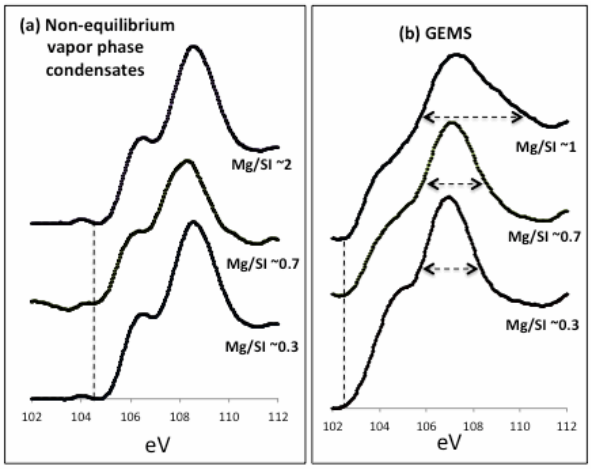

Figure 1: *Silicon L core scattering edges (background-subtracted and smoothed) from (a) non-equilibrium MgSiOx vapor phase condensates, (b) GEMS in CP IDP U220A19 for various Mg/Si ratios.*

Results: Silicon L-edges from condensed MgSiOx grains with a range of Mg/Si atomic ratios are plotted in Figure 1a. In all cases, onset of the edge is at ~105 eV and there is little variation in the near edge structure. Silicon L-edges from the GEMS are significantly

different (Figure 1b). Onset of the edges is ~2 eV lower than the vapor condensed silicates, and both the fine structure and broadness of the peaks change with Mg/Si ratio. (The edges also show a slight shift to lower energies with decreasing Mg/Si ratio).

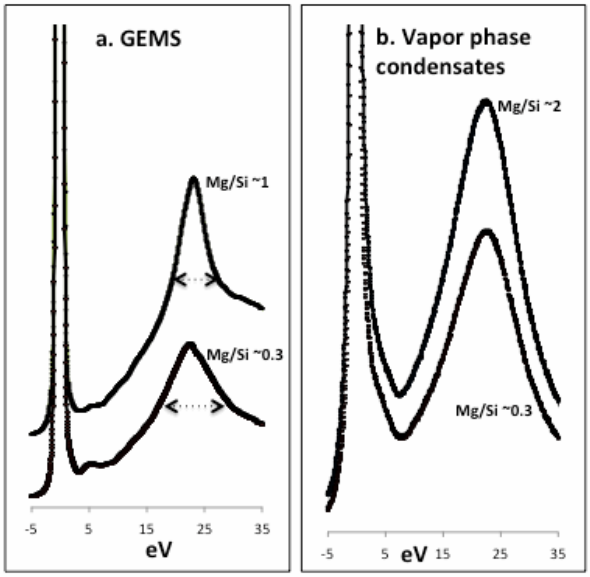

Figure 2: *Low-loss features from (a) two non-equilibrium MgSiOx vapor phase condensate grains, and (b) two GEMS in CP IDP U220A19.*

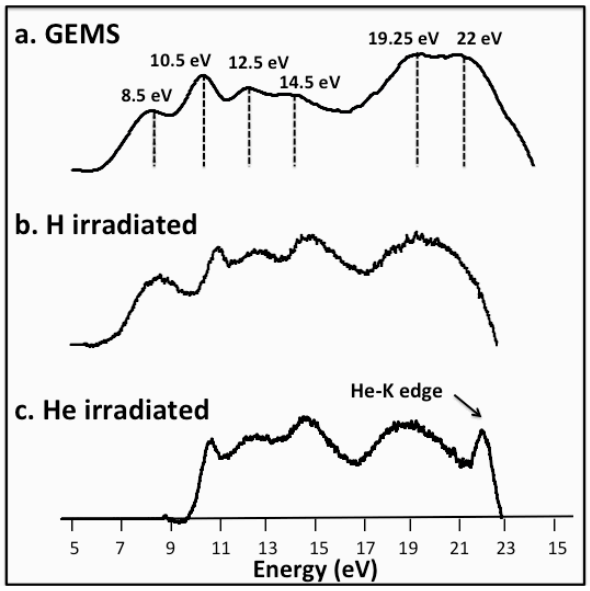

Figure 3: *Derivative spectra of the 5-25 eV plasmon region of (a) a GEMS grain in CP IDP U220A19, and amorphous silicates produced by exposing San Carlos olivine to (b) 5 keV H^{2+} at a fluence of ~10^{19}/cm and (c) 5 keV He^{+} ions at a fluence of ~10^{18}/cm^2*

The low-loss features of non-equilibrium vapor phase condensates and GEMS are shown in Figure 2. The most notable feature of the GEMS plasmons is a decreased broadness with decreasing Mg/Si ratio (Fig. 2a). In contrast, the broadness of the plasmon peaks from the vapor phase condensates is relatively insensitive to Mg/Si ratios (Fig. 2b).

There are other differences in the plasmon peaks from GEMS and vapor phase condensate grains examined to date: Plasmon peaks from the condensates are featureless, but those from several GEMS examined thus far exhibit detailed fine structure. Figure 3a shows a derivative spectrum of the low-energy (5-25 eV) side of the plasmon peak of a low-Mg (Mg/Si <0.5) GEMS. Superimposed on the plasmon are fine structures with peaks at ~8.5, 10.25, 12.5, 14.4, 19.2 and 21 eV. Interestingly, matching features are present in amorphous silicates produced by H and He-irradiation of San Carlos olivine (Figs 3b & c).

Discussion: The Si $L_{2,3}$-edge results from dipole allowed transitions from a core 2p state to unoccupied states with s- and d-like character [9]. For the vapor phase condensates, the positions and shapes of the Si $L_{2,3}$ edges (Fig. 1a) and plasmon peaks (Fig. 2b) appear to be typical of amorphous Mg silicates in general [2,9]. The edges and plasmons from GEMS are more complicated (Figs 1b & 2a). Changes in the Si $L_{2,3}$ edges imply that local atomic arrangments and degree of short-range order vary with Mg/Si ratio in GEMS (Fig. 1b). In irradiation-produced amorphous silicates, Mg/Si ratios decrease with increasing damage [10]. Fine structure peaks on the plasmon peaks from GEMS analyzed to date are also observed on irradiation-produced amorphous silicates [4,11], strongly suggestive of irradiation in the histories of GEMS. Ongoing HREELS studies will lay the groundwork for distinguishing these and additional mechanisms for amorphous silicate formation.

References: [1] Gilbert B. et al. (2003) *Am. Min., 88,* 763-769. [2] Garvie L. and Buseck P.R. (1994) *Am. Min., 84,* 946-964. [3] Erni R. et al. (2005) *Micron* 36, 369-379. [4] Bradley, J.P. and Dai, Z.R. (2009) *MAPS* 44, 1627-1642. [5] Brink, H.A. (2003) *Ultramicroscopy* 96, 367-384. [6] Nuth, J.A. (2002) MAPS 37, 1579-1590. [7] Bradley, J.P. (1994) *GCA* 58, 2123-2134. [8] Brownlee D.E. et al. (1999) *LPSC* Abs. 2031. [9] Hansen P.L. et al. (1992) *Microsc. Microanal. Microstruct*. 3, 213-219. [10] Bradley, J.P. (1994) *Science* 265, 925-929. [11] Hojou, K. et al. (1998) *Nucl. Instr Methods* B141, 148-153.

This work was supported by NNH11AQ88I (Cosmochemistry) to JPB. Portions of this work were performed under the auspices of US DOE by LLNL under Contract DE-AC52-07NA27344.